Advanced Eigenbeamforming for the 3GPP UMTS FDD Downlink

Ralf Seeger and Karl-Dirk Kammeyer
Department of Communications Engineering
University of Bremen
Otto-Hahn-Allee 1, 28359 Bremen, Germany
Email: {seeger, kammeyer}@ant.uni-bremen.de

Thomas Hindelang and Wen Xu
Siemens AG - Mobile Phones
Grillparzer Str. 10-18, 81675 Munich, Germany
Email: {Thomas.Hindelang, Wen.Xu}@siemens.com

Abstract— In this paper, the 3GPP downlink eigenbeamformer scheme is investigated. The eigenbeamformer scheme performs an eigendecomposition (EVD) of the spatial long-term covariance matrix to obtain beamforming weights. Diversity gains are obtained due to switching between so-called eigenbeams. Since the EVD is carried out by the mobile station, computationally efficient algorithms are required. We show that the computational efforts can be drastically reduced by exploiting the quasi-stationarity of the long-term spatial covariance. For a given feedback rate, the performance of closed-loop schemes drop at high velocities due to delay introduced by feedback of side information. To cope with this problem, an efficient spatio-temporal prediction scheme is proposed. Our simulations, in which realistic coding, feedback delay, channel estimation and quantization of eigenbeams are considered, show that for a given target block error rate, the operational range, i.e. the maximally allowed speed of the mobile station, can then be significantly increased. Furthermore, measurements with our hardware demonstrator are used to study eigenbeamforming under realistic propagation conditions.

I. INTRODUCTION

Future mobile and wireless applications such as multimedia services will require significantly higher data rates, better QoS and lower costs as compared to current systems. With conventional single antenna systems, it is usually difficult to meet these high requirements on data rate, link quality, spectral efficiency, and mobility. Therefore, antenna arrays will be employed at least at the base station (BS). Due to the asymmetric nature of most data services (internet downloads, broadcast services) there is a demand on increased downlink capacity. Several multiple-input multiple-output (MIMO) and transmit diversity concepts are currently proposed to 3GPP for standardization. While MIMO schemes imply multiple antennas at both ends of a transmission link to increase the throughput, transmit diversity schemes and/or beamforming schemes which intend to raise the signal-to-noise-and-interference ratio (SINR) at the mobile station (MS) generally require only one receive antenna, thus being attractive to build low cost mobile stations. In this paper we focus on the downlink eigenbeamformer scheme [1] which is based on [2]. The beamforming weights are obtained by an eigendecomposition (EVD) of the spatial long-term covariance matrix. Since the EVD is performed by the MS, highly efficient algorithms are necessary. We will show in Sec. III-A that the computational complexity can be drastically reduced by exploiting the quasi-stationarity of the long-term spatial covariance [3].

Fading, especially flat fading, is one of the main reasons to affect the downlink capacity. In order to improve this, spatial diversity can be exploited by switching between weight vectors (eigenbeams) [1]. For a given feedback rate, the performance of closed-loop schemes drops at higher velocities due to limited uplink bandwidth in connection with a delay involved in the feedback of side information [4]. To cope with loop delays, an efficient spatio-temporal prediction scheme is proposed in Sec. III-B. We will show by simulation including channel estimation and quantization of eigenbeams that the operational range, i.e. the maximal allowed speed of the MS for a given target block error rate (BLER), can then be significantly increased.

In addition measurements with our hardware demonstrator are undertaken to study eigenbeamforming under realistic propagation conditions. Despite of the quite simple measurement setup a first impression of available gains due to adaptive transmit beamforming are obtained.

II. SPATIAL CHANNEL MODEL

In [5][6], stochastic multiple-input-multiple-output (MIMO) radio channel models are derived from the classical tap delay line model that is based on the wide-sense stationary uncorrelated scattering (WSSUS) assumption where L independent time-varying taps model the signal dispersion in a multipath environment. Let the BS have M transmit antennas. The tap fading process is extended by incorporating long-term spatial correlations ρ_{m_1,m_2} between the signals from different transmit antennas m_1 and m_2. The matrix capturing all spatial correlation coefficients for tap l is denoted by $\mathbf{R}_l \in \mathbb{C}^{M \times M}$. It is assumed that the M signals from the antennas associated with tap delay l arrive simultaneously at the MS. The channel coefficients of different antennas m at delay l, $h_{l,m}$, can be modeled by a linear combination of M independent normalized complex Gaussian processes $\mathbf{g}_l(t) = [g_{l,1}(t), g_{l,2}(t), \ldots, g_{l,M}(t)]^T$ with required power density spectrum, leading to

$$\mathbf{h}_l(t) = \mathbf{R}_l^{1/2} \mathbf{g}_l(t). \tag{1}$$

The projection matrix $\mathbf{R}_l^{1/2} \in \mathbb{C}^{M \times M}$ is obtained using a standard matrix square root decomposition method $\mathbf{R}_l = \mathbf{R}_l^{1/2}\mathbf{R}_l^{1/2H}$ [7, p.149].

Assume that at the BS the antenna weights $\mathbf{w}^* = [w_1^*(t), w_2^*(t), \ldots, w_M^*(t)]^T$ are applied [8], then the signal received at the MS (after descrambling and despreading), which is equipped with one receive antenna, can be written as

$$r(t) = \sum_{l=1}^{L}[\mathbf{w}^H s(t - \tau_l)]\mathbf{h}_l(t) + n(t), \qquad (2)$$

where $s(t)$ is the dedicated user signal prior to spreading and scrambling, and $n(t)$ denotes the additive white Gaussian noise (AWGN).

Using the channel model described in [5], the normalized long-term spatial correlation matrix is given by the superposition of time discrete micro paths components which cannot be resolved by the receiver

$$\mathbf{R}_l = \frac{1}{\sigma_l} \sum_{\mu \in \mathcal{L}_l} \sigma_\mu \mathbf{a}(\phi_\mu, \theta_\mu)\mathbf{a}^H(\phi_\mu, \theta_\mu), \qquad (3)$$

where $\mathcal{L}_l$, $\mathbf{a}(\phi_\mu, \theta_\mu)$ denote a class of non-resolvable micro paths associated with the temporal tap l, the steering vector as a function of direction of departure (DOD) in azimuth ϕ and elevation θ, respectively. The power per micro path is denoted by σ_μ, and total power of superposed paths is denoted by σ_l. It is assumed that the long-term properties behave quasi-stationary (magnitudes, angles-of-departure changes very slowly over several 100 ms).

III. 3GPP EIGENBEAMFORMING SCHEME

The main idea behind the eigenbeamformer method is the decomposition of the directional fading channel (2) into it's fundamental processes in order to provide a decorrelation of spatial diversity branches (see [1][2]). Using orthogonal common pilot sequences (CPICHs) transmitted from the BS, the MS estimates the short-term spatial covariance matrix averaged over the temporal taps of the channel. In the sequel we will restrict to the flat fading case to simplify the signal model. Therefore, omitting the temporal tap index l from (1) the short-term spatial covariance can be calculated as follows:

$$\mathbf{R}_{ST}(k) = \mathbf{h}(k)\mathbf{h}^H(k), \qquad (4)$$

where k is the time slot index. The long-term spatial covariance matrix is obtained by averaging over the short-term covariance matrices applying the forgetting factor ρ

$$\mathbf{R}(k) = \rho\mathbf{R}(k-1) + (1-\rho)\mathbf{R}_{ST}(k). \qquad (5)$$

In general it is reasonable to assume a spatially quasi-stationary environment (the long-term covariance is nearly constant over several 100 time slots [9]), consequently the forgetting factor ρ is set close to unity. Decorrelation in space is achieved by an eigenanalysis of the Hermitian matrix $\mathbf{R}$
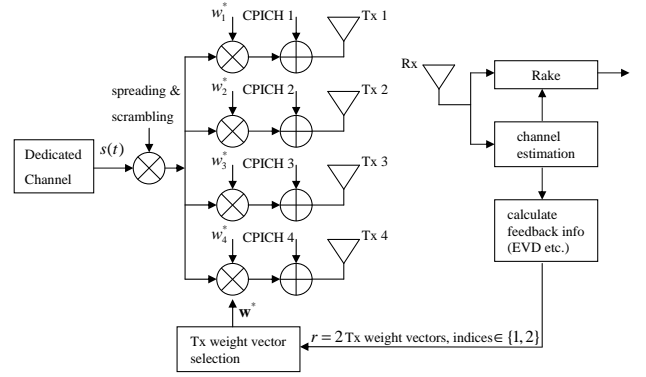

Fig. 1: 3GPP eigenbeamforming scheme according to [1]

$$\mathbf{RW} = \mathbf{WD}, \qquad (6)$$

where the orthonormal column vectors $\mathbf{w}_m$ of $\mathbf{W}$ are eigenvectors (in the sequel termed *eigenbeams*) of $\mathbf{R}$ and $\mathbf{D} = diag[d_1, d_2, \ldots, d_M]$ is a diagonal matrix with the corresponding eigenvalues. Without loss of generality we assume $d_1 > d_2 > \ldots > d_r > \ldots > d_M$.

A subset of the strongest r eigenbeams out of M eigenbeams is fed back to the BS. Exploiting the quasi stationary of the long-term parameter (3) the feedback bits are distributed over a large number of slots. In addition, a slot-by-slot selection of the strongest eigenbeam is performed by the MS according to

$$\mathbf{w}_{\max}(k) = \arg\max_{\mathbf{w}_m}(\mathbf{w}_m^H(k)\mathbf{R}_{ST}(k)\mathbf{w}_m(k)), \qquad (7)$$

i.e., the eigenbeam $\mathbf{w}_m$ that maximizes the receive signal power is selected and the index m is sent to the BS which applies the corresponding eigenbeam after some delay (see Fig. 1).

A. Tracking the Eigenbeams

The benefit of the 3GPP downlink eigenbeamforming scheme is that, since the eigenbeams are calculated by the MS, diversity can be gained by beam-switching. On the other hand the eigendecomposition must be performed at the MS which has normally tight energy constraints (small battery supply) in connection with reduced computational capabilities. In this section we propose computationally efficient EVD algorithms, which exploit the quasi-stationary property of spatial long-term covariance matrix to *track* the eigenspace.

In contrast to batch EVD methods like the symmetric QR-algorithm the following algorithms can make use of the eigenvectors calculated from past time slots as an approximation of the current one, based on the assumption that the spatial covariance changes very slowly with time. Note, although we will use the time slot index k in the sequel, the eigendecomposition is practically performed only once every several 100 ms up to one second [4]. Concrete update rates will be discussed in Section IV.

1) Jacobi algorithm: The Jacobi algorithm is one possible method to solve the symmetric eigenvalue problem (6). The idea behind the Jacobi algorithm is to systematically reduce the energy stored in off-diagonal elements and shift it to the main diagonal elements [7]. This iterative diagonalization is done by Jacobi rotations (unitary transforms) $\mathbf{J}_i(k) \in \mathbb{C}^{M \times M}$

$$\mathbf{W}(k) = \prod_i \mathbf{J}_i(k),$$
$$\mathbf{D}(k) = \mathbf{W}^H(k)\mathbf{R}(\mathbf{k})\mathbf{W}(k), \tag{8}$$

where the approximated eigenspace $\mathbf{W}(k)$ of $\mathbf{R}(\mathbf{k})$ is the product of all previously applied rotations, and i the iteration index. The Jacobi rotation is defined by:

$$\mathbf{J}_i(k) =$$

$$
\begin{array}{cc}
 & \begin{array}{ccc} \quad p & \quad\quad\quad q \end{array} \\
\begin{array}{c} \\ \\ p \\ \\ q \\ \\ \\ \end{array} &
\left[
\begin{array}{ccccccc}
1 & \dots & 0 & \dots & 0 & \dots & 0 \\
\vdots & \ddots & \vdots & & \vdots & & \vdots \\
0 & \dots & \cos(\phi)e^{j\varphi} & \dots & \sin(\phi)e^{j\varphi} & \dots & 0 \\
\vdots & & \vdots & \ddots & \vdots & & \vdots \\
0 & \dots & -\sin(\phi) & \dots & \cos(\phi) & \dots & 0 \\
\vdots & & \vdots & & \vdots & \ddots & \vdots \\
0 & \dots & 0 & \dots & 0 & \dots & 1
\end{array}
\right]
\end{array} . \tag{9}
$$

The basic step in the Jacobi eigenvalue procedure involves computing a cosine-sine pair (9). The term $e^{j\varphi}$ is chosen such that the diagonalization of the 2-by-2 submatrix from $\mathbf{R}$ reduces to a real symmetric problem and the symmetric Schur decomposition [7, p.427] can be used to calculate $\cos(\phi)$ and $\sin(\phi)$. The index pair (p, q) is chosen in a row-by-row manner (cyclic Jacobi method) to avoid searching the off-diagonal elements with maximal squared magnitude at the cost of slightly reduced convergence speed. The Hermitian property of matrix $\mathbf{R}$ is sustained by unitary transformations, therefore, cycling through the upper or lower triangular of $\mathbf{R}$ is sufficient. After $M(M-1)/2$ iterations (called one *sweep*) each off-diagonal element is zeroed once. Note that consecutive rotations will destroy previously obtained zeros. There is no rigorous theory to predict the number of sweeps that are required to a specific reduction of the off-diagonal norm. On the other hand, the number of sweeps can be decreased to reduce the computational complexity depending on the application [10]. We will show by simulation that one sweep is sufficient exploiting the quasi-stationary property of the spatial covariance matrix. The previously calculated product sum of rotation matrices $\mathbf{W}(k-1)$ is a good approximation of the eigenspace of the updated $\mathbf{R}(k)$ (5). Therefore, it is beneficial to apply the Jacobi iterations on the *pre-multiplied* version of the spatial covariance matrix, i.e. replacing $\mathbf{R}(k)$ with $\tilde{\mathbf{R}}(k)$ in (8) [11]:

$$\tilde{\mathbf{R}}(k) = \mathbf{W}^H(k-1)\mathbf{R}(k)\mathbf{W}(k-1). \tag{10}$$

The Jacobi method does not directly incorporate the rank-one update of the spatial covariance matrix into the EVD process (as specialized subspace tracking algorithms do, e.g. [12]) and runs independently of (5), therefore, the algorithm may not overwrite $\mathbf{R}(k)$ directly, instead it iterates over a *copy* of $\mathbf{R}(k)$.

2) Orthogonal Iteration: The so called *orthogonal iteration* is a straightforward extension of the well-known power method. If $r = 1$ holds, the sequence of estimated eigenvectors by the orthogonal iteration method is precisely the sequence of vectors produced by the power method [7, p.410]. The algorithm is outlined as follows:

$$\mathbf{Q}_0 = \mathbf{W}_r(k-1)$$
for $i = 1, 2, \dots, i_{\max}$ **do**
$\quad \mathbf{Z}_i(k) = \mathbf{R}(k)\mathbf{Q}_{i-1}(k)$
$\quad \mathbf{Q}_i(k)\mathbf{R}_{QR}(k) = \mathbf{Z}_i(k) \qquad$ (QR-decomposition)
end for
$\mathbf{W}_r(k) = \mathbf{Q}_{i_{\max}}(k)$

TABLE I: Orthogonal iteration method based on dimensionally reduced QR-decomposition. Previously calculated eigenvectors of the slowly time-varying spatial covariance are used for initialization of the iteration loop at each EVD update step.

The matrix $\mathbf{W}_r \in \mathbb{C}^{M \times r}$ consists of the first r column vectors of $\mathbf{W}$. At the first time $k = 0$, $\mathbf{W}_r(-1)$ is initialized with an arbitrary orthonormal matrix, e.g. the first r columns of unity matrix. The dimensionally reduced QR-decomposition is the core function of orthogonal iteration. Implementation variants of the QR-decomposition are discussed in [13].

Normally, for most applications sophisticated acceleration strategies such as Ritz acceleration and shifting are needed to make the orthogonal iteration method applicable [7, p.422].

Regardless the poor convergence properties, we found that for the eigenbeamforming scheme no further enhancements of the algorithm in Tab. I are required. Furthermore, with the same arguments as for the Jacobi tracking method we can state that $\mathbf{W}_r(k-1)$ is a good approximation of the (dimensionally reduced) eigenspace of $\mathbf{R}(k)$ since the spatial covariance changes very slowly with time. Therefore, $\mathbf{Q}_0 = \mathbf{W}_r(k-1)$ is a good starting choice to provide fast enough convergence. Instead of using $i_{\max} = 4$ iterations for the power method applied in [4] only 1 iteration is required as shown in Section IV.

3) Computational Complexity and Numerical Stability of EVD Algorithms: The Jacobi algorithm has an inherent parallel structure and therefore, it is suited for hardware implementation like specialized signal processor cores, which performs the elementary rotations in hardware [14]. The complete eigenspace instead of a subset of strongest eigenvectors is computed. Moreover, the eigenvalues and -vectors calculated by the cyclic Jacobi algorithm are not sorted. Therefore, additional computational effort is needed to get the r strongest eigenvectors used by the eigenbeamforming scheme. The two-sided multiplication with $\mathbf{W}$ in (10) takes $2(M^3 + (M-1)M^2)$

complex operations (multiplications and additions) for the Jacobi algorithm, whereas in case of the orthogonal iteration only multiplication with $\mathbf{W}_r \in \mathbb{C}^{M \times r}$ is required (see Table I) taking only $rM^2 + (M-1)Mr$ operations. The QR-decomposition based on Householder transformation takes $4(M^2 r - Mr^2 + r^3/3)$ operations; in contrast, the Jacobi method roughly takes $2M^3$ operations per sweep [7].

Note that the given complexity counts are only rough estimates, when square root or inverse trigonometric functions required to implement Jacobi rotations is neglected. However, some special implementation techniques, e.g. approximated Jacobi rotation, exist [14]. Table II summarizes the results from above discussion.

Beside its low computational complexity, the favored orthogonal iteration method based on elementary Householder reflections offers excellent numerical properties, i.e. it is numerical stable (see references in [13][7]).

B. Predictive Beam-Switching

According to [1] the downlink eigenbeamformer scheme selects the eigenbeam which maximizes the *expected* instantaneous signal-to-noise ratio (7). To do so, the MS transmits the corresponding beam-index to the BS, which applies the desired transmit weight vector after some processing delay. In addition to the measurement delay, i.e. the MS calculates the short-term feedback information based on the already received slot, up to two delay slots must be considered due to uplink transmission and some processing delay at the BS. Consequently, for high MS velocities the applied transmit weights are outdated due to fast channel fluctuations. In the following, the total amount of delay (in slots) is denoted as *loop delay* κ.

We can conclude from the underlying channel model that the temporal short-term processing for the eigenbeam selection can be analyzed independently from the spatial long-term processing. To cope with the loop delay the channel coefficients in (7) can be replaced by *predicted* channel coefficients obtained from a bank of M mutually independent linear complex-valued predictors (i.i.d. temporal fading processes are assumed in (1)). Let $\mathbf{h}(k+\kappa|k)$ denote the predicted channel coefficient vector in the current slot k for the future slot $k+\kappa$, we obtain from (7):

$$\mathbf{w}_{\max} = \arg \max_{\mathbf{w}_m} (\mathbf{w}_m^H \mathbf{h}(k+\kappa|k)\mathbf{h}^H(k+\kappa|k)\mathbf{w}_m), \quad (11)$$

with
$$m = 1, 2, \ldots, M.$$

However, in the multiple-input-single-output (MISO) case, channel estimation has to be performed for all M spatial paths in order to calculate the spatial covariance. Nevertheless, the MS can exploit the set of calculated eigenvectors *after* channel estimation to reduce the complexity of consecutive short-term processing. We are enabled to apply matrix multiplication with $\mathbf{W}$ prior to the temporal prediction scheme

$$\tilde{\mathbf{h}}(k) = \mathbf{W}_r^H \mathbf{h}(k), \quad (12)$$

where the dimensionally reduced channel coefficient vector is denoted by $\tilde{\mathbf{h}} = [\tilde{h}_1, \tilde{h}_2, \ldots, \tilde{h}_r]^T$.

By constraining the r predictors to be linear FIR filters of order $N_p - 1$, the output of the r predictors at time slot k can be described as follows

$$\begin{bmatrix} \tilde{h}_1(k+\kappa|k) \\ \tilde{h}_2(k+\kappa|k) \\ \vdots \\ \tilde{h}_r(k+\kappa|k) \end{bmatrix} = \begin{bmatrix} \mathbf{p}_1 & & & \\ & \mathbf{p}_2 & & \\ & & \ddots & \\ & & & \mathbf{p}_r \end{bmatrix}^H \begin{bmatrix} \tilde{h}_1(k) \\ \tilde{h}_1(k-1) \\ \vdots \\ \tilde{h}_1(k-N_p-1) \\ \tilde{h}_2(k) \\ \tilde{h}_2(k-1) \\ \vdots \\ \tilde{h}_2(k-N_p-1) \\ \tilde{h}_r(k) \\ \tilde{h}_r(k-1) \\ \vdots \\ \tilde{h}_r(k-N_p-1) \end{bmatrix},$$

(13)

where $\mathbf{p} \in \mathbb{C}^{N_p \times 1}$ are the coefficient vectors associated with the r predictors. Therefore, (11) simplifies to

$$m_{r_{\max}} = \arg \max_{m_r} (\tilde{h}_{m_r}^*(k+\kappa|k)\tilde{h}_{m_r}(k+\kappa|k)), \quad (14)$$

with
$$m_r = 1, 2, \ldots, r.$$

As mentioned above, spatially uncorrelated coefficients $\tilde{h}_{m_r}$ can be obtained with (12), if (6) holds. Then, we are able to determine the prediction filter coefficients for each of the r predictors separately. According to the minimum mean-square-error (MMSE) criterion, the optimal weight vector is obtained from the solution of the Wiener-Hopf equation :

$$\mathbf{R}_{m_r} \mathbf{p}_{m_r} = \mathbf{r}_{m_r}, \quad (15)$$

where $\mathbf{R}_{m_r} \in \mathbb{C}^{N_p \times N_p}$ and $\mathbf{r}_{m_r} \in \mathbb{C}^{N_p \times 1}$ are the *temporal* autocorrelation matrix and vector, respectively [15]. To determine $\mathbf{R}_{m_r}$ and $\mathbf{r}_{m_r}$ the vector $\tilde{\mathbf{h}}'_{m_r} = [\tilde{h}_{m_r}(k-\kappa), \tilde{h}_{m_r}(k-\kappa-1), \ldots, \tilde{h}_{m_r}(k-\kappa-N_p+1)]^T$ is defined. It follows

$$\mathbf{R}_{m_r} = E\{\tilde{\mathbf{h}}'_{m_r}\tilde{\mathbf{h}}'^H_{m_r}\}, \quad (16)$$
$$\mathbf{r}_{m_r} = E\{\tilde{h}_{m_r}^*(k)\tilde{\mathbf{h}}'_{m_r}\}, \quad (17)$$

where $E\{\cdot\}$ denotes the expectation, which can be practically calculated analogical to (5) assuming quasi-stationary temporal fading processes. Thus exploiting the Toeplitz structure of $\mathbf{R}_{m_r}$ the Levinson-Durbin algorithm can be used to solve (15), or alternatively, the Trench algorithm can be applied to directly compute the matrix inversion. Both algorithms exhibit $\mathcal{O}(N_p^2)$ computational complexity [7]. Note that the explicit estimation of autocorrelation $\mathbf{R}_{m_r}$ matrix is required. This takes additional $\mathcal{O}(N_p^2)$ operations. In order to

EVD algorithm	flops	$M = 4, r = 2$
Batch EVD (Symmetric QR)	$9M^3$	576
Jacobi (1 sweep)	$2M^3 + 2(M^3 + (M-1)M^2)$	352
orthogonal iteration (1 iteration)	$4(M^2r - Mr^2 + r^3/3) + rM^2 + (M-1)Mr$	131

TABLE II: Number of complex-valued operations. For the Jacobi method the two-sided pre-multiplication (10) is included. Since an EVD takes place e.g. only once per second (1500 slots), the number of operations per slot is very low.

avoid explicit calculation of (inverse) autocorrelation matrix, the RLS algorithm with $\mathcal{O}(N_p^2)$ complexity can be employed [15]. Eq. (14) implies an absolute square operation after linear prediction, thus the *power* predictor is nonlinear. The authors of [16] pointed out that the employed kind of power predictor is optimal in the MMSE sense if the bias is removed according to [16, Eq.(11)]. However, we found out by simulation (not shown in this paper) that the bias removal does not observably improve the results presented in Sec. IV.

IV. SIMULATION RESULTS

In order to evaluate the discussed algorithms, some simulations were conducted. Since we are interested in an overall performance of the communication system, the bit error rates (BERs) instead of mean-square-error results are used to evaluate the subspace tracking algorithms. The transmit power is normalized to the number of transmit antennas and $E\{\sum_l |h_{l,m}(t)|^2\} = 1$ holds.

According to [1] $M = 4$ Tx antennas and switching between two, $r = 2$, eigenbeams are assumed. The array geometry is set to uniform linear array (ULA), which is also the reference topology in [17], with half-wavelength spacing. One user with a bit rate of $240\,\mathrm{kbit/s}$ (spreading factor 32) is considered. The total power of the common pilot channels equals to the power of the dedicated channel. All downlink intracell interferer are mutually orthogonal since flat fading is assumed.

The prediction scheme consists of two predictors of order 10, and the RLS algorithm is used to adapt the filter coefficients.

The batch EVD and Jacobi algorithm were initialized with the unity matrix, whereas for the orthogonal iteration method the first $r = 2$ columns were used to initialize $\mathbf{W}$. The number of iterations (resp. sweeps) is set to 1 for the orthogonal iteration and Jacobi algorithm. Since the feedback rate in a UMTS Rel. 99 system is fixed to one bit per uplink slot, there is a trade-off between the eigenspace update rate and the number of bits per eigenvector, which affects the spatial resolution. A detailed analysis is, however, out of the scope of this paper.

The eigenvectors are quantized by using 3 bits for the phase argument and 2 bits for the magnitude part of a complex number. According to [1], one long-term bit and 14 short-term bits are fed back every frame (15 slots). It has to be mentioned that errors during uplink transmission of feedback bits may occur. Consequently, additional redundancy for the long-term bits and antenna weight verification is indispensable for practical systems [8]. Here error-free uplink transmission is assumed. A code rate of $r_c = 1/2$ for the long-term bits and one antenna as phase reference are used. The EVD update rate
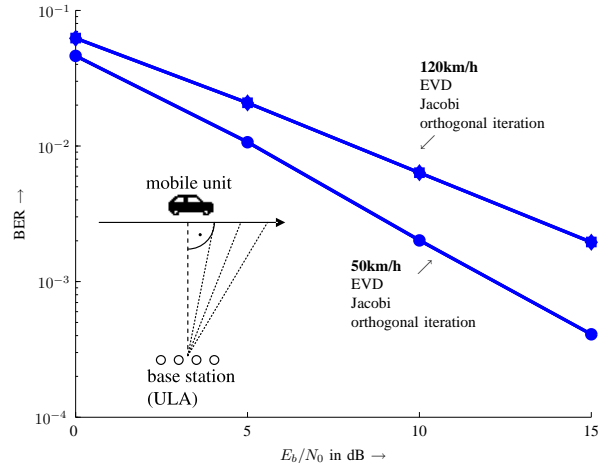

Fig. 2: Spatially quasi-stationary environment: the MS moves parallel w.r.t. the BS antenna array axis. The angle spread is fixed to $30°$, therefore, this corresponds to a spatially highly correlated case with one dominant eigenvalue. The distance between the MS and the BS is set to $500\,\mathrm{m}$ (perpendicular to the array axis).

is $680\,\mathrm{ms}$ (i.e. $(3 \cdot 3\mathrm{bit\ phase} + 4 \cdot 2\mathrm{bit\ amplitude}) \cdot 2\mathrm{beams} \cdot 1/r_c \cdot 10\,\mathrm{ms}$).

In the spatially quasi-stationary scenario, where the MS moves on a trajectory as depicted by Fig. 2, no difference between tracking and batch EVD is noticed. However, the computational complexity can be drastically reduced compared to the standard batch EVD method. The orthogonal iteration yields nearly the same performance at the lowest computational cost. Note that ideally known channel state information is assumed.

Next, we compare the conventional eigenbeamformer scheme proposed to 3GPP [1] to the enhanced version incorporating subspace tracking *and* predictive beam-selection. The spatially stationary *Microcell* scenario defined in [18] is used. Channel estimation based on the mutually orthogonal common pilot channels is performed. We simply average the pilot symbols over one slot, since a Wiener smoothing filter spanning over multiple slots would contribute an additional processing delay. It can be seen that the reduced dimensional prediction scheme (14) exhibits slightly better performance compared to the conventional prediction scheme, and much less computational complexity, i.e. 2 instead of 4 predictors are required (see Fig. 3).

In realistic communication systems coded transmission is employed. Therefore, one important figure of merit for link level simulations is the BLER. The applied convolutional
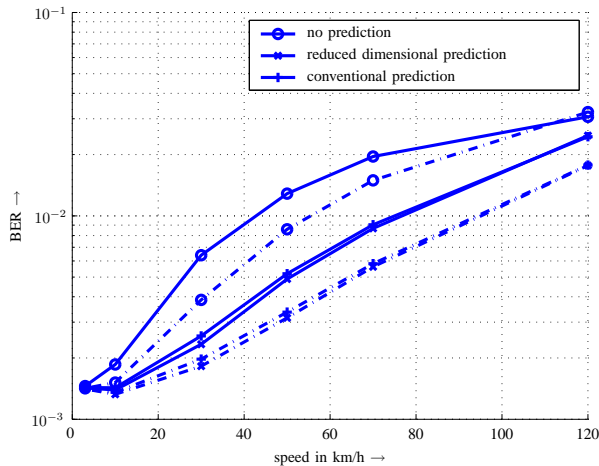
Fig. 3: *Microcell* environment with fixed $E_b/N_0 = 10$ dB. The eigenbeamformer uses eigenbeam tracking based on orthogonal iteration and predictive beam-switching. The loop delay is set to 2 (dash-dot lines) and 3 (solid lines).
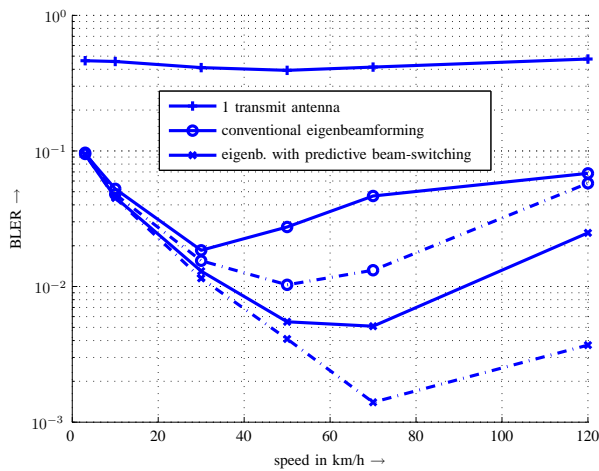

Fig. 4: Coded system performance: BLER vs. speed, $E_b/N_0 = 4$ dB, *Microcell* environment. Both eigenbeamforming schemes employ eigenbeam tracking based on orthogonal iteration, whereas the proposed enhanced scheme benefits from predictive beam-switching. The loop delay is set to 2 (dash-dot lines) and 3 (solid lines).

encoder (with rate $r_c = 1/2$) and the intra and inter frame interleavers were implemented according to [19]. The transmission time interval (TTI) is set to 20 ms (i.e. two frames per block). At the receiver a Max-Log-MAP-Decoder is applied for decoding [20]. All other parameters are left unchanged regarding to the uncoded system described above. In Fig. 4 BLERs for a system with one Tx antenna, the conventional and the proposed enhanced predictive eigenbeamforming scheme are depicted. The subspace tracking scheme based on orthogonal iteration from Sec. III-A is used. The predictive eigenbeamforming scheme yields the lowest BLERs over the whole range of considered speeds. For a fixed speed of the MS an significant signal-to-noise gain can be obtained as it can be seen from Fig. 5.
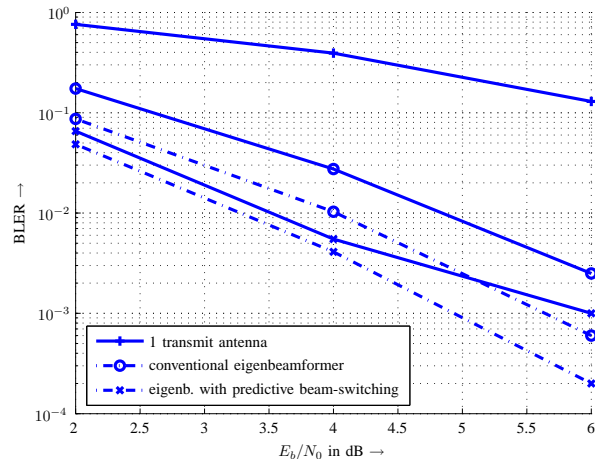

Fig. 5: Coded system performance: BLER vs. E_b/N_0, 50 km/h. The loop delay is set to 2 (dash-dot lines) and 3 (solid lines).

V. MEASUREMENTS

To assess multiple antenna systems it is indispensable to study the propagation aspects, i.e. to verify commonly applied (statistical) assumptions made about the MIMO radio channel. The objective of our MIMO hardware demonstrator is to evaluate MIMO algorithms under non-idealized environments deploying common hardware components. Moreover, thanks to selectable frontend processing we are not restricted to a specific radio interface standard.

A. A Multiple Antenna System for ISM-Band Transmission

The top-level system is diagrammed in Fig. 6. At the workstation environment in-phase and quadrature (I/Q) data, e.g. UMTS frames, are generated by the simulation system of choice. The impulse shaping is done in the digital domain. The data is scaled and quantized to meet the hardware demonstrator concerns and finally stored into a file. Due to its wide distribution the USB interface is chosen to connect the hardware demonstrator with the workstation. To transfer the I/Q data via the USB interface we use a customized application software which allows us to set several parameters, like sample rate (from external or internal clock), local oscillator (LO) frequency tuning value and assignment of data files to corresponding antennas. Furthermore, in a Matlab environment we can directly access the demonstrator by calling a Matlab function [21]. This is useful for fully automated measurements. Inside the demonstrator the I/Q data is stored into digital buffers which are addressed in a circular manner: the increment pointers for memory accesses wrap to the beginning of the buffer when its end is reached. The currently addressed I/Q words are fed to a digital-to-analog converter (DAC), whose analog baseband output signals drive the radio frequency (RF) stage, which performs up-conversion to the desired RF frequency band.

At the receiver, the RF passband signal is down-converted to the complex baseband and analog-to-digital converted. A
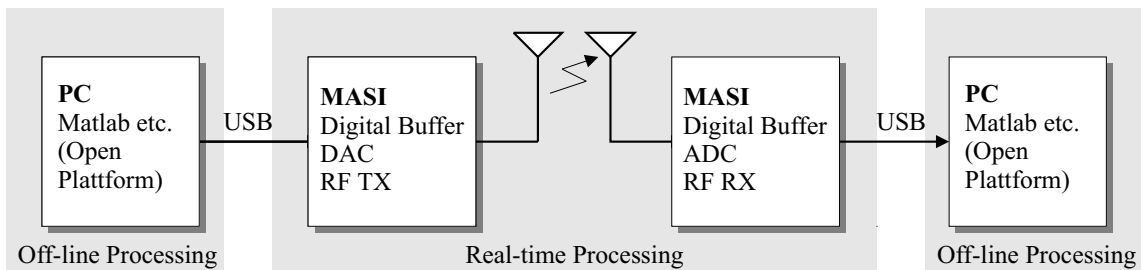
Fig. 6: Principle block diagram of the Multiple Antenna System for ISM-band Transmission (MASI).

Fig. 7: The Multiple Antenna Transmitter for ISM-Band Transmission equipped with 8 modules.

snapshot is stored into a digital buffer. Because frame synchronization is not implemented in hardware the receive buffer has a length twice as large as that of the transmit buffer to ensure that at least one complete frame is captured. The sample rate is adjustable up to 80 MHz and may be chosen from a set of internally predefined frequencies or an external source. The request for extensibility of the hardware demonstrator led to a modular architecture; for each antenna the connected transmitter or receiver hardware has its own plug-in module (see Fig. 7). The digital clock and LO signal is provided to all modules by a central clock base to ensure inter module synchronization of sample rate and carrier phase.

However, as a fixed sampling clock is used which is not synchronized to the transmitter clock, symbol timing and carrier recovery have to be accomplished. This is done offline in the digital domain. A more detailed of employed components and already conducted measurements are given in [22].

B. Eigenbeamforming

To assess the eigenbeamforming scheme under real propagation scenarios we conducted a couple of simple measurements.

The number of antennas, used common pilot channels and spreading factors are the same as in Sec. IV. The measurements were performed in an indoor environment, i.e. we transmitted between two adjacent office rooms of approx. 20 sqm size each. The total transmit power per antenna was 17 dBm (50 mW).

Since full-duplex wireless transmission is currently not supported the existing wired local area network (LAN) infrastructure is used to realize the feedback channel (uplink). In contrast to previously discussed eigenbeamforming schemes only the strongest eigenbeam is fed back, i.e. fast slot-by-slot beam-switching is not accomplished. The eigenvector is updated every 3 seconds. The measurements are conducted in a relative static environment, i.e. the transmitter and receiver are placed at fixed positions inside the office rooms. However, in case of a non-idealized static scenario e.g with persons sitting inside the office rooms we observed a slightly changing beamforming vector (Fig. 8). A remarkable increased SNR due to eigenbeamforming can be observed as depicted in Fig. 8 and Fig. 9. One has to emphasize that only one arbitrary specific spatial scenario is presented here. In general any positive gain w.r.t. to the 1 transmit antenna case can be observed depending on the positions of the transmit antennas and the receive antenna. However, this quite simple measurement scenario gives a first impression of gains available from adaptive transmit beamforming.

VI. CONCLUSIONS

We studied the 3GPP eigenbeamforming scheme with realistic feedback delay, quantization of eigenbeams and channel estimation in spatially stationary and quasi-stationary environments. The conventional scheme exhibits a strong degradation for relatively high mobile station velocities. It was shown that due to the predictive short-term processing based on the efficient spatio-temporal prediction scheme, a velocity of $70 \, \text{km/h}$ and a fixed signal-to-noise ratio of $E_b/N_0 = 4 \, \text{dB}$, the BLER is lowered from $1.3 \cdot 10^{-2} (4.7 \cdot 10^{-2})$ to $1.4 \cdot 10^{-3} (5.1 \cdot 10^{-3})$ for a loop delay of 2 (3) slots. It can be concluded that for a given BER/BLER the operational range, i.e. the maximally allowed speed of the mobile station, can be significantly increased. Furthermore, we have shown, by exploiting the quasi-stationarity of the spatial covariance matrix, that the proposed eigenbeam tracking scheme can lower the computational costs considerable. In addition measurements
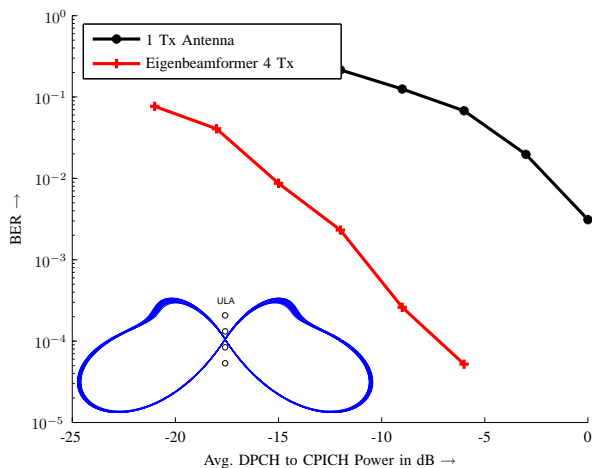
Fig. 8: BER vs. transmit power of the dedicated channel (DPCH). One measured channel realization (transmitter and receiver are placed at fixed positions). The power of the common pilot channels (CPICHs) is left constant. 16-QAM is used. In addition the corresponding beam pattern is included.
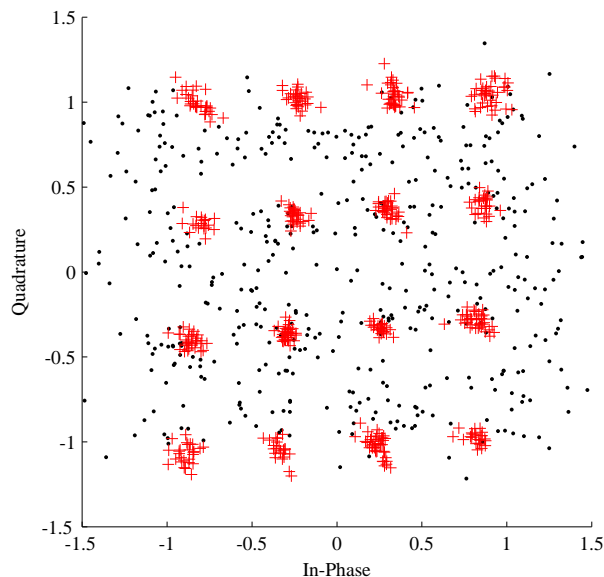

Fig. 9: 16-QAM signal constellation after Rake combiner (same setup as for Fig. 8). The 1 transmit antenna scheme (dots) and the eigenbeamformer using 4 transmit antennas (pluses) are depicted.

with our hardware demonstrator were accomplished to study eigenbeamforming under realistic propagation conditions. This quite simple measurement scenario give a first impression of gains available from adaptive transmit beamforming.

REFERENCES

[1] 3GPP, "Tx diversity solutions for multiple antennas," in *3GPP technical report, 3G TR25.869 V1.0.0*, 2002.
[2] C. Brunner, *Efficient Space-Time Processing Schemes for WCDMA*, Ph.D. thesis, TU München, 2000.
[3] I.J. Viering, *Analysis of Second Order Statistics for Improved Channel Estimation in Wireless Communications*, Ph.D. thesis, University of Ulm, Germany, 2003.
[4] A.Seeger, A.Lobinger, R.Wiedmann, and B.Raaf, "Performance of Downlink Eigenbeamformer with Realistic Feedback Transmission," in *Proc. IEEE VTC Fall*, 2001.
[5] J.S. Hammerschmidt and A.A. Hutter, "Spatio-Temporal Channel Models for the Mobile Station: Concept, Parameters, and Canonical Implementation," in *Proc. IEEE VTC Spring, Tokyo*, May 2000.
[6] K.I. Pedersen, J.B. Andersen, J.P. Kermoal, and P.E. Mogensen, "A Stochastic Multiple-Input-Multiple-Output Radio Channel Model for Evaluation of Space-Time Coding Algorithms," in *Proc. IEEE VTC Fall*, 2000, vol. 2, pp. 893–897,.
[7] G.H. Golub and C.F. van Loan, *Matrix Computation*, The John Hopkins University Press, Baltimore, 3rd edition, 1996.
[8] A. Seeger, M. Sikora, and W. Utschick, "Antenna Weight Verification for Closed-Loop Downlink Eigenbeamforming," in *Proc. IEEE Global Telecommunications Conference, Taipei, Taiwan*, 2002.
[9] 3GPP TSG RAN1, "Description of the eigenbeamformer concept (update) and performance evaluation," in *TSGR1#19 R1-01-0203*, Las Vegas, USA, February 27- March 2, 2001.
[10] J. Götze, "Monitoring the Stage of Diagonalization in Jacobi Type Methods," in *Proc. IEEE ICASSP*, 1994, vol. 3, pp. 441–444.
[11] C. Michalke, M. Stege, F. Schäfer, and G. Fettweis, "Efficient Tracking of Eigenspaces and its Application to Eigenbeamforming," in *Proc. IEEE PIMRC*, 2003, vol. 3, pp. 2847–2851.
[12] B. Yang, "Projection Approximation Subspace Tracking," *IEEE Trans. Signal Processing*, vol. 43, no. 1, pp. 95–107, Jan. 1995.
[13] R.B. Lehoucq, "The Computation of Elementary Unitary Matrices (LA-PACK Working Note 72)," *http://www.netlib.org/lapack/lawns*, October 1995.
[14] J. Götze, "On the Parallel Implementation of Jacobi and Kogbetliantz Algorithms," *SIAM J. Scientific Computing*, vol. 15, no. 6, pp. 1331–1348, 1994.
[15] S. Haykin, *Adaptive Filter Theory*, Prentice Hall, 4th edition, 2001.
[16] T. Ekman, M. Sternad, and A. Ahlén, "Unbiased Power Prediction of Rayleigh Fading Channels," in *Proc. IEEE VTC Fall*, 2002.
[17] 3GPP, "Spatial channel model for Multiple Input Multiple Output (MIMO) simulations," in *3GPP technical report, 3G TR25.996 V6.1.0*, 2003.
[18] 3GPP TSG RAN1, "Simulation parameters for Tx diversity simulations using correlated antennas," in *TSGR1#16 R1-00-1180*, October 10-13, 2000, Pusan, Korea.
[19] 3GPP, "Multiplexing and channel coding (FDD)," in *3GPP technical specification, 3G TR25.212 V6.2.0*, 2004.
[20] S. Benedetto, G. Montorsi, D. Divsalar, and F.Pollara, "Soft-Output Decoding Algorithms in Iterative Decoding of Turbo Codes," *The TDA Progress Report. Pasadena, CA: Jet Propulsion Lab.*, vol. 42-124, pp. 63–87, 1996.
[21] K.D. Kammeyer and V. Kühn, *Matlab in der Nachrichtentechnik*, Informations- und Kommunikationstechnik. J. Schlembach-Verlag, Weil der Stadt, Germany, 1. edition, 2001.
[22] J. Rinas, R. Seeger, L. Brötje, S. Vogeler, T. Haase, and K.D. Kammeyer, "A Multiple-Antenna System for ISM-Band Transmission," *EURASIP Journal on Applied Signal Processing - Special Issue on Advances in Smart Antennas*, , no. 9, pp. 407–1419, Aug. 2004.